Available online at www.sciencedirect.com
SCIENCE DIRECT®
Thermochimica Acta 432 (2005) 229–240
thermochimica acta
www.elsevier.com/locate/tca

Fast determination of evaporation enthalpies of solvents and binary mixtures using a microsilicon chip device with integrated thin film transducers☆

G.A. Groß, J.M. Köhler*

Technical University of Ilmenau, Institute of Physics, Department of Physical Chemistry and Microreaction Technology, Weimarer Straße 32, D-98693 Ilmenau, Germany

Received 10 December 2004; received in revised form 8 March 2005; accepted 10 March 2005
Available online 23 May 2005

Abstract

A silicon chip device with two types of integrated platinum thin film resistors was applied for microcaloric measurements. It was shown that the device is capable of fast characterization of liquid evaporation behaviour and allows the determination of evaporation enthalpies for pure liquids and mixtures. The applicability was demonstrated for a wide range of solvents from nonpolar aliphatic solvents over polar organics to protic solvents (e.g. *iso*-octane, toluene, acetone, ethanol, methanol and water). The sample volumes were in the range of about 2–5 μL. The determination of transient times, in case of constant power mode, or the power integral over time was used for the fast estimation of binary liquid mixtures. Thermo-resistive measurements of 5 μL droplets of solvent mixtures like methanol/*iso*-propanol, ethanol/water, *iso*-octane/*iso*-propanol and *iso*-octane/1,4-dioxane showed significant changes in temperature characteristics and evaporation enthalpies in dependence on composition. The applied heating power was about 1 W, which corresponds to measurement times between a few seconds and a minute.

Keywords: Microcalorimetry; Chip calorimeter; Solvent evaporation; Binary mixtures; Thin film transducers

1. Introduction

Chip reactors and other miniaturized chemical devices are under development for analytical and synthetical applications. They are applied in so-called μ-TAS systems and are essential for the lab-on-chip concept [1–4]. Chip-based reactors play an increasing role in the development of new chemical procedures and are of particular interest for the determination of molecular information. That is why, chip technology has been introduced in molecular biology namely DNA techniques [5–13]. Combinatorial chemistry and high-throughput screening [14,15] applications are also of great interest in that context.

Microchannel reactors are predominantly applied for continuous flow processes [16–20] but also for serial flow processes like segmented flow operations [21–27]. Liquid handling processes can be realized in such channels without open liquid surfaces. Thus, the evaporation of liquids is significantly suppressed or completely avoided by the reactor walls. But, in case of highly parallelized operations like combinatorial chemistry and high-throughput screening applications, parallel carriers are much more favourable than microchannel reactors. These microtiterplates (MTP) and nanotiterplates (NTP) are used in large extend. This type of carrier allows a parallel handling of about 10^2 to 10^4 samples in parallel, whereby the individual samples can be identified and operated using a simple spatial *x*/*y*-addressing [28,29]. Usually, single vials are filled by liquid dispensing. Additionally, aliquots of samples are removed by micropipetting in some cases. A major problem of this operation mode is the

☆ This paper was not presented at the 8th Lahnwitzseminar on Calorimetry.
* Corresponding author. Tel.: +49 3677 69 3629; fax: +49 3677 69 3179.
E-mail address: michael.koehler@tu-ilmenau.de (J.M. Köhler).

0040-6031/$ – see front matter © 2005 Elsevier B.V. All rights reserved.
doi:10.1016/j.tca.2005.03.019

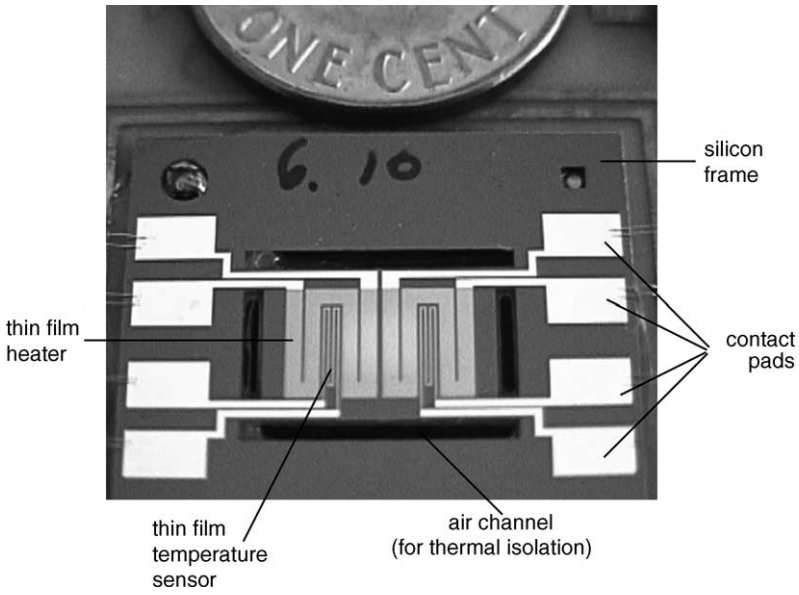

Fig. 1. Chip carrier with integrated thin film transducers for microevaporation experiments.

lost of solvent by evaporation caused by the open liquid surface. The loss of solvent due to evaporation is not negligible because of the high surface to volume ratios. This problem becomes still more important, if the sample volume is reduced from microlitres (MTP formats) to nanolitres (NTP formats). It was shown that the complete evaporation from nanotiterplates with chamber volumes of about 150 nL takes place in a few minutes [30,31]. Therefore, the knowledge of evaporation behaviour and the availability of methods for the miniaturized determination of evaporation rates is essential for parallelized chemical processes in MTPs and NTPs. In most cases evaporation enthalpies are well known for pure solvents [32]. In addition, miniaturized methods and devices are needed for a fast determination of evaporation rates and evaporation enthalpies for mixtures. Therefore, a simple device and fast method for the temperature-dependent measurement of evaporation and the estimation of evaporation enthalpies of pure substances and binary mixtures is reported.

2. Experimental

All experiments were carried out using a silicon device as microcalorimetric carrier. This device is microlithographically prepared from a 4 inch silicon wafer. The configuration of the device corresponds to chip reactors developed earlier for the application of miniaturized DNA amplification by PCR [9].

A well with a depth of 0.4 mm is placed at the centre of the chip (Fig. 1). Into this well, the liquids are applied for

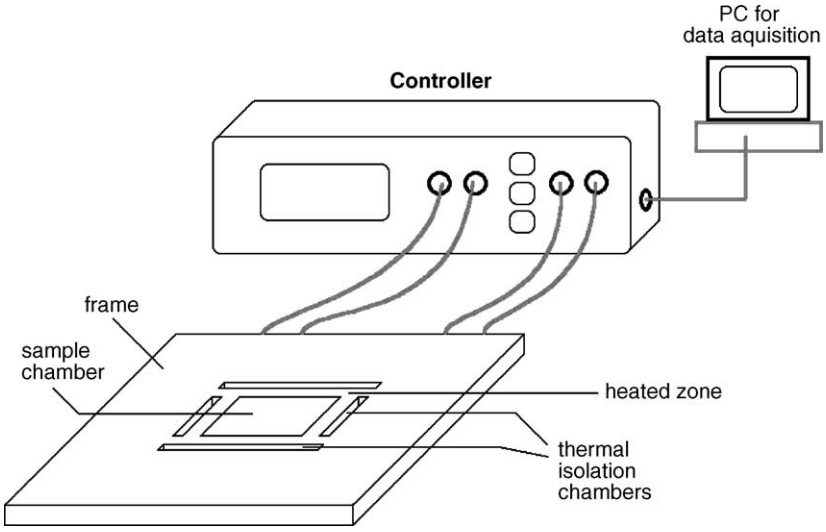

Fig. 2. Experimental set-up for microevaporation experiments.

investigation. It is possible to apply substance volumes up to 10 μL. Two thin film resistors with low electrical resistance for heating and two separate thin film transducers for thermoresistive temperature measurement are integrated at the back side of these well. The metal films are electrically insulated by a thin dielectric layer (Si_3N_4) of 1 μm thickness. These support thickness allows a fast heat transfer between the metal films and the silicon despite the low heat conductivity of silicon nitride. The bottom of the sample well is formed by a silicon membrane of about 100 μm thickness. This membrane also supports a fast heat transfer due to the high heat conductivity of silicon. The sample well is surrounded by four trenches in the silicon chip. These trenches are necessary for the thermal separation of the central area of chip device and its frame. In this way, the temperature gradients are focused in the region of these trenches and the remaining small silicon beams, respectively. The thermal conduction inside the sample area is high. The heat transfer from the sample area to the surrounding area is lower, but fast enough for electronic temperature control by a feedback loop control. The thermal time constants of the central region with the sample well are less then 1 s and allows fast measurement procedures. Monocrystalline silicon (double side-polished wafer) was applied for the body of the device. Thin films of dielectric material (SiO_2 and Si_3N_4) were used for the lithographical process and as insulating layer. These films were deposited by chemical vapour deposition. The metal thin films were deposited by sputtering and micropatterned by sputter etching. The silicon was anisotropically etched by alkaline etching bathes using Si_3N_4 masks. All micropatterns were generated photolithographically using novolak-based photoresists.

The experimental set-up is shown in Fig. 2. A self-constructed electronic controller was used for the read-out of temperatures and the control of heating power. The device allows measurements at constant temperature and at constant power. In both cases, the actual temperature and the heating power were registered with a rate of 2 Hz using a PC with AD interface. All used chemicals were graded for analysis.

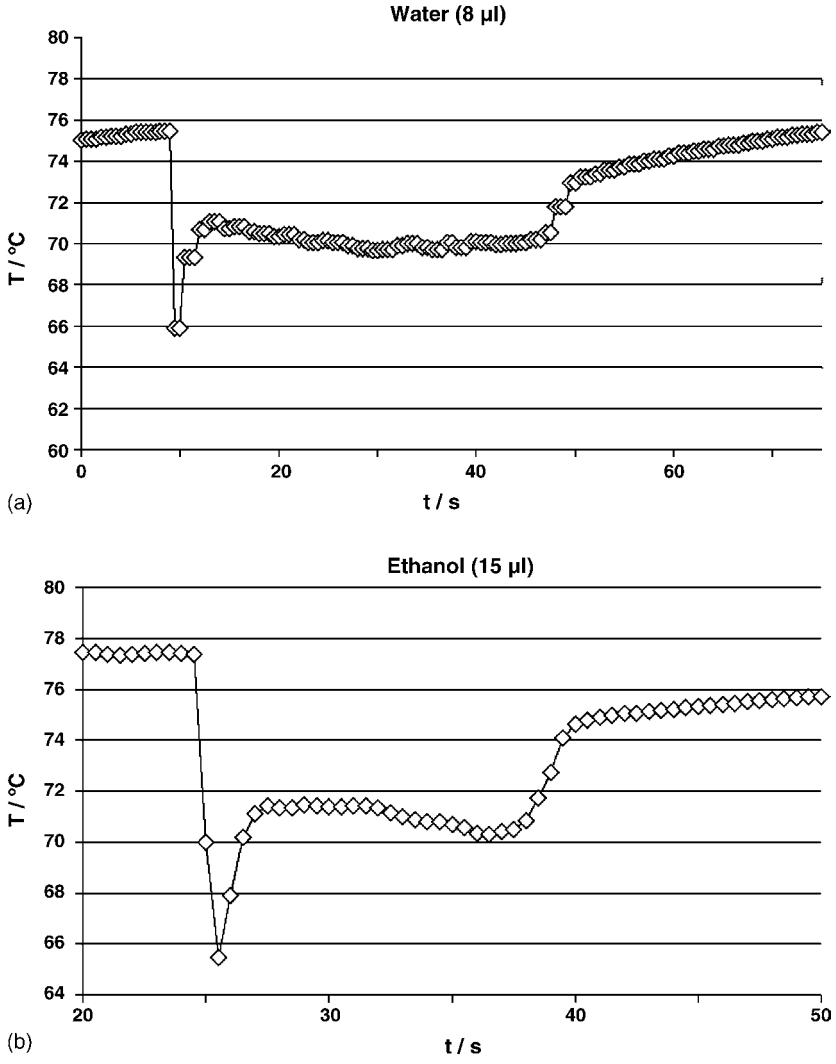

Fig. 3. Temperature signal during pipetting and evaporation of a water droplet: (a) 8 μL; (b) 15 μL measured at constant heating power of 1.4 W.

The solvent drops were placed in the sample well using microdispensers or directly by pipetting.

3. Results and discussion

3.1. Evaporation of water and ethanol droplets at constant heating power

The chip device allows an easy observation of the process of evaporation. For this purpose the device is heated with a certain electrical power. Droplets of appropriate liquids are placed in the sample well after a constant temperature was reached. A decrease of temperature is always detectable by the answer in the temperature-related thin film resistance due to the heat capacitance of the samples and the heat loss due to the liquid evaporation. If a 8 μL water drop was applied at a heating power of 1.4 W and a corresponding start temperature of about 75 °C a fast temperature drop of about 10 K was observed (Fig. 3a). The first temperature transient takes about 1.5 s and was assigned for heating-up the droplet. The following temperature transient has a duration of about 80 s, but the temperature drop is small (about 5 K). This transient is caused by the evaporation. At the end of the transient phase, the liquid is completely evaporated.

A similar first transient was observed for the evaporation of 15 μL ethanol, when a temperature range close to the boiling point was chosen (Fig. 3b). The temperature drop about 12 K in this case and the transition time was about 1 s. In contrast to water, the second transient time was only 12 s despite the larger volume. This behaviour is due to the much lower evaporation enthalpy and lower boiling temperature of ethanol, respectively, the ethanol/water azeotrope in comparison with pure water. The temperature transient shows a slight minimum at the end of the transition phase (Fig. 3b), which is explained by a temperature gradient in the liquid during the evaporation process. The heating energy must be conducted from the silicon–liquid interface to the liquid surface. This distance is reduced by the volume loss during the evaporation and becomes smallest in the last phase of the evaporation process. Hence, it is to assume that in this last phase the highest temperature gradient and the most efficient heat transfer from the transducer to the liquid surface take place resulting in a moderate additional decrease of device temperature. The reproducibility of measurements of ethanol evaporation is reflected by Fig. 4.

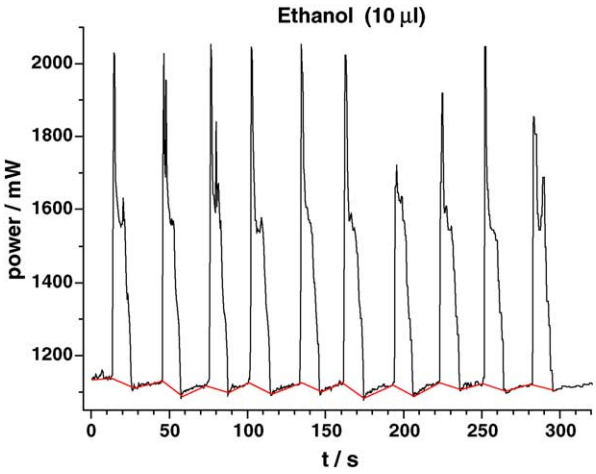

Fig. 4. Power consumption signal during the pipetting and evaporation of ethanol droplets (10 μL) measured at constant temperature mode (input heating power between 1 and 2.0 W).

Both, the temperature drop and the length of transition phase is reduced when the droplet volume decreases. Fig. 5 shows the application of a series of droplets with decreasing volume (20–3 μL) on the chip device at constant power. In all cases a characteristic start peak and a typical broad minimum in the longer transition region was observed. The transition time is reduced monotonous with decreasing vol-

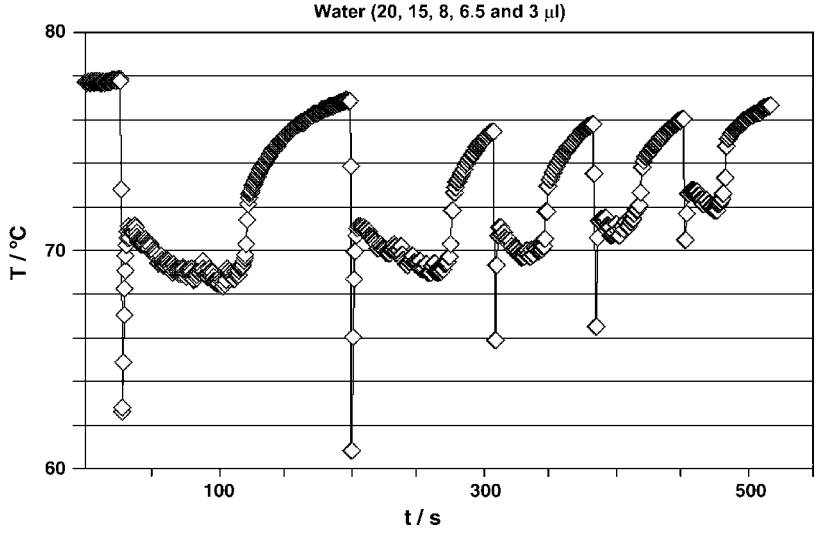

Fig. 5. Temperature signals during the pipetting and evaporation of water droplets. Measured at constant power mode of 1.4 W and different droplet size.

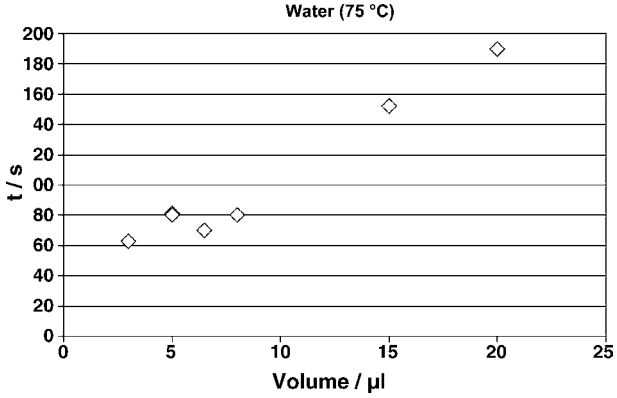

Fig. 6. Dependence of evaporation time measured at constant power mode of 1.4 W and different droplet volumes.

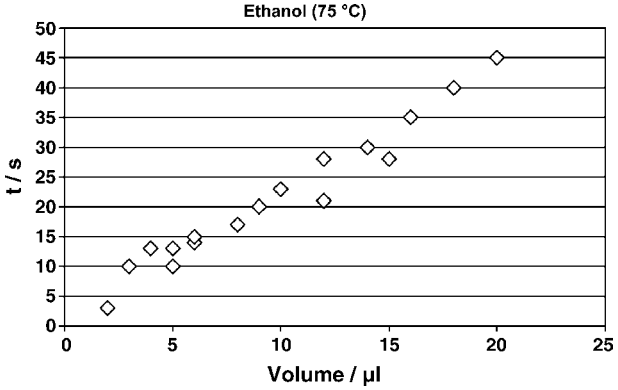

Fig. 8. Dependence of the evaporation time of water droplets measured at constant power mode of 1.4 W and different droplet volumes.

ume. This fact suggests that the transition time rather than the temperature drop indicates the consumed evaporation heat. Therefore, the transition time can be used for the estimation of the original size of the droplets (Fig. 6). The shrinkage of ethanol droplets leads to the analogous signals (Fig. 7). The transition time is continuously reduced from 22.5 s in case of 20 μL ethanol down to 1.5 s for 2 μL droplets. There is a linear dependence between evaporation time and the droplet volume (Fig. 8). Obviously, not the liquid surface but the volume is crucial for the duration of the evaporation process. That means that the evaporation enthalpy determines the duration of the process.

The application of 5 μL of a high concentrated KCl solution (3 mol/L) results in small negative temperature drop and in a longer temperature transient, as observed in case of pure water. The temperature difference during the transition time was about 3 K. This value was significantly smaller then the temperature drop in case of 5 μL pure water (5 K) at the same heating power. After a typical evaporation time of about 40 s for this volume a third temperature transition was found, when salt-containing aqueous solutions were investigated. The temperature drop during this transition was only about 1 K, but the third transition phase had a length of about 80 s (Fig. 9). The total of the integral of the second and third transition phase (about 120 + 80 K s) is approximately equal to the integral of the second transition signal of 5 μL pure water (about 5 K × 40 s = 200 K s).

This was interpreted as a reduction of needed evaporation power due to the lower vapour pressure during the second transition period and a slow evaporation of salt-bonded water possessing a strongly reduced vapour pressure in the third transition phase.

3.2. Estimation of evaporation enthalpies for different solvents through isothermal measurements

The evaporation behaviour of different organic solvents was studied through isothermal measurements. The chip device was controlled at 60 °C for these measurements. Different solvents were chosen for these experiments and varied from alkanes (nonpolar solvents) and acetone (polar aprotic solvent) to protic solvents (alcohols). The

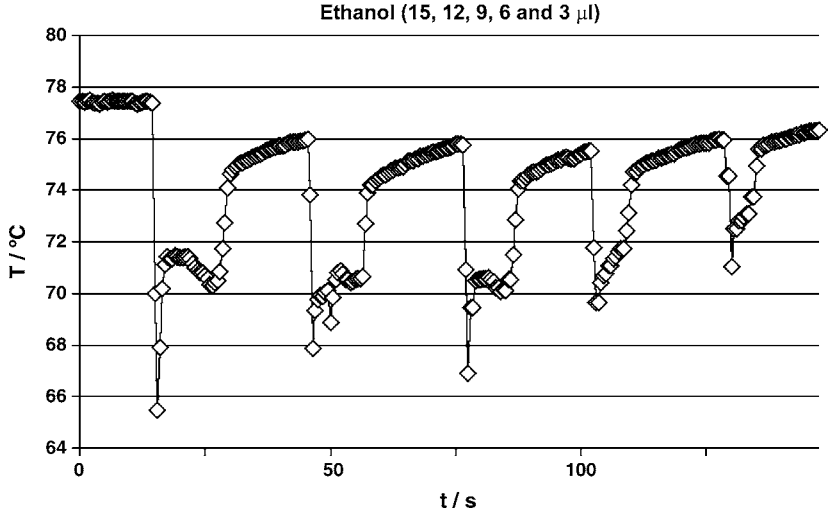

Fig. 7. Temperature signals during the evaporation of ethanol droplets measured at constant power mode of 1.4 W and different droplet volumes.

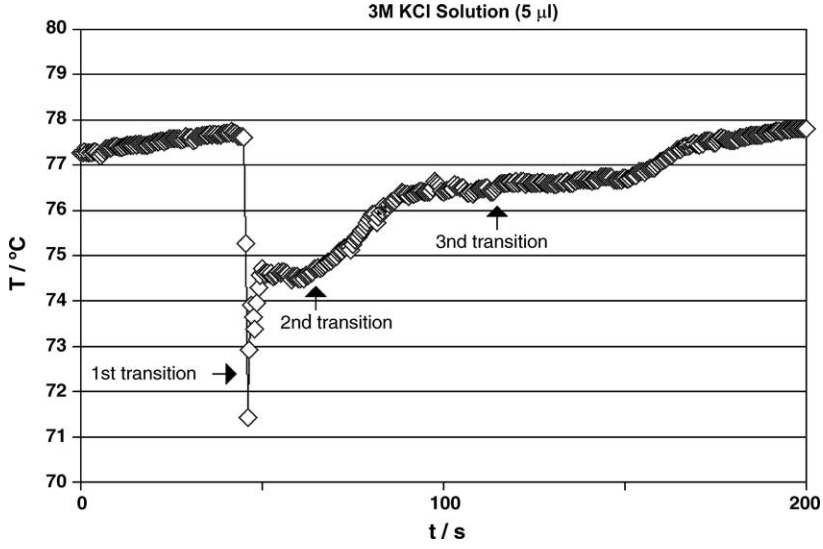

Fig. 9. Transient temperature signal during pipetting and evaporation of a 5 μL droplet of concentrated KCl solution (3 mol/L) during constant heating with 1.4 W.

Table 1
Examples of solvents: boiling temperatures and evaporation enthalpies [32]

Substance	Formula	Boiling point (°C)	ΔH_m (molar) (kJ/mol)	ΔH_{sp} (specific) (J/g)	ΔH_{vol}^{tab} (volume-related) (J/ml)	ΔH_{vol}[a] (volume-related) (J/ml)
iso-Octane	C_8H_{18}	113.1	32.7	286	201	161
Toluene	C_7H_8	110.6	33.5	364	317	256
Acetone	C_3H_6O	56.1	29.1	501	396	228
Dioxane	$C_4H_8O_2$	101.6	35.8	406	420	–
iso-Propanol	C_3H_8O	82.5	40.5	674	529	450
Ethanol	C_2H_6O	78.4	38.7	840	667	547
Methanol	CH_4O	64.6	35.4	1105	879	467
Water	H_2O	100	40.66	2259	2259	1886

[a] Average of three measurements, determined with the chip calorimeter.

solvents are distinguished by different molecular size and molecular interactions resulting in considerably different boiling temperatures and specific evaporation enthalpies (Table 1).

There were different characteristics for the power consumption after application of solvent droplets onto the microdevice. The power consumption and the resulting energy during the transition states – that means the duration of com-

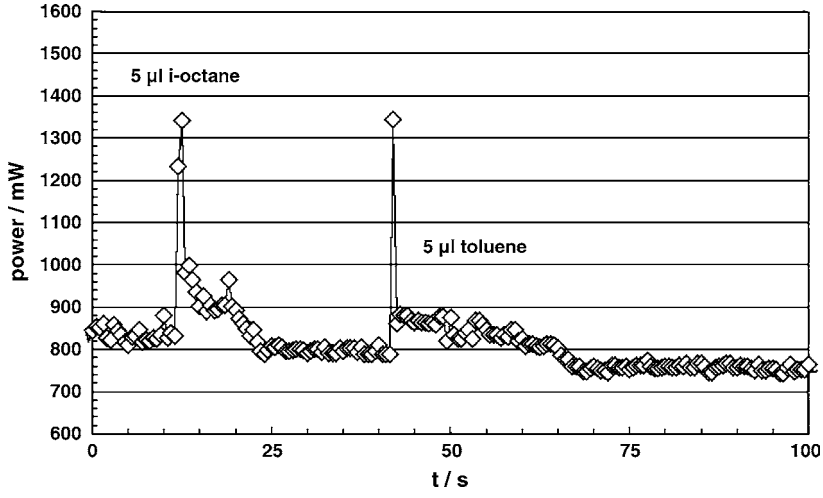

Fig. 10. Power consumption of two solvents with comparatively high vapour pressure at temperature-controlled evaporation conditions (quasi-isothermal) at 60 °C.

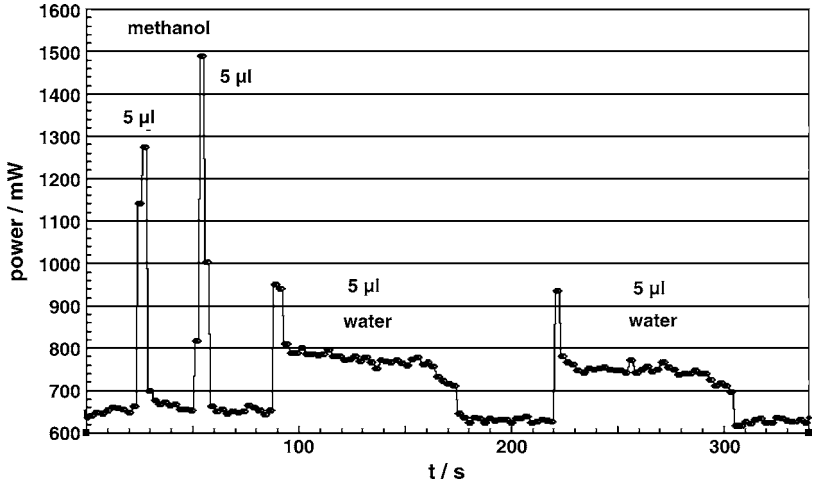

Fig. 11. Power consumption of methanol and water droplets under temperature-controlled evaporation conditions (quasi-isothermal) at 60 °C.

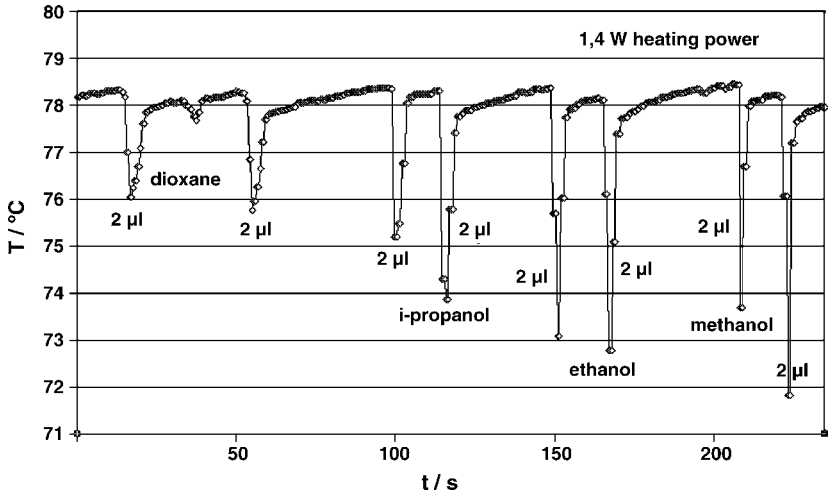

Fig. 12. Transient temperature signal during pipetting and evaporation of 2 µL droplets of different solvents measured at constant power mode of 1.4 W.

plete evaporation multiplied by the power enhancement – are determined by the vapour pressure on the one hand and the evaporation enthalpy on the other hand. Accordingly, *iso*-octane as well as toluene showed a slight power increase only. For *iso*-octane a significant shorter evaporation time was observed as for toluene (Fig. 10). Clearly this is due to the considerably lower volume-related evaporation enthalpy of *iso*-octane in comparison with toluene.

Even more significant behaviour was found during the comparison between methanol and water (Fig. 11). The boiling temperature of methanol is much lower than the boiling temperature of water. Methanol possesses a much higher vapour pressure than water. The volume-related evaporation enthalpy of methanol is considerably lower than the water one. This leads to a steep increase of power needed for keeping the temperature constant after the application of methanol (Fig. 11, first two peaks). But the power transient was short because of the high evaporation rate of methanol. The evaporation of water was much more time consuming (Fig. 11, last two peaks). When the evaporation was studied under constant power mode, an increase in the temperature drop was observed with decreasing boiling point (Fig. 12).

The power consumption was used for the estimation of the enthalpies of the different solvents. Fig. 13 shows that

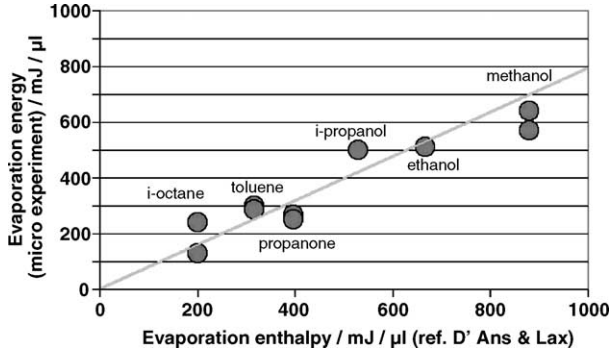

Fig. 13. Consumed heating energy during the evaporation of different solvents (5 µL) in dependence on their volume related evaporation enthalpies (data taken from [32]).

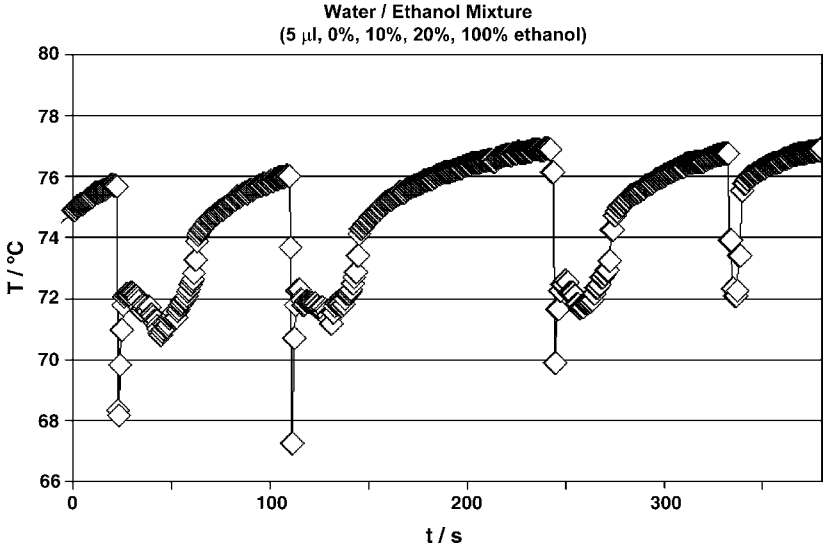

Fig. 14. Evaporation of binary mixtures: transient temperature signals during the pipetting and evaporation of 5 μL droplets of a binary solvent mixture (water and ethanol) under constant power conditions (1.4 W).

variation in the additional heating energies during the transition phases corresponds to the volume-related evaporation enthalpies known from literature. The additional power consumption during evaporation was found to fall below the value expected from the known evaporation enthalpies. This effect is probably due to the reduction of parasitic energy loss from the electrically heated microdevice in the presence of droplets. The isothermal measurement with the microdevice results better data for the estimation of evaporation enthalpies than measurements at constant heating power.

3.3. Microevaporation experiments with binary solvent mixtures

The temperature drop, transition times as well as the integral of additional power need not only be used for

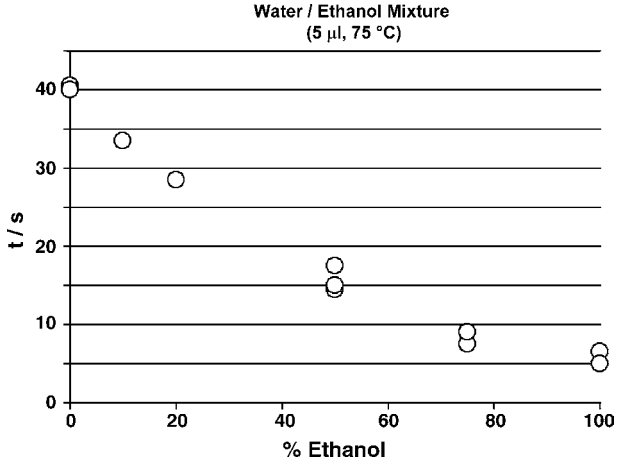

Fig. 15. Evaporation time of 5 μL droplets of aqueous ethanol mixtures measured in constant temperature mode (75 °C).

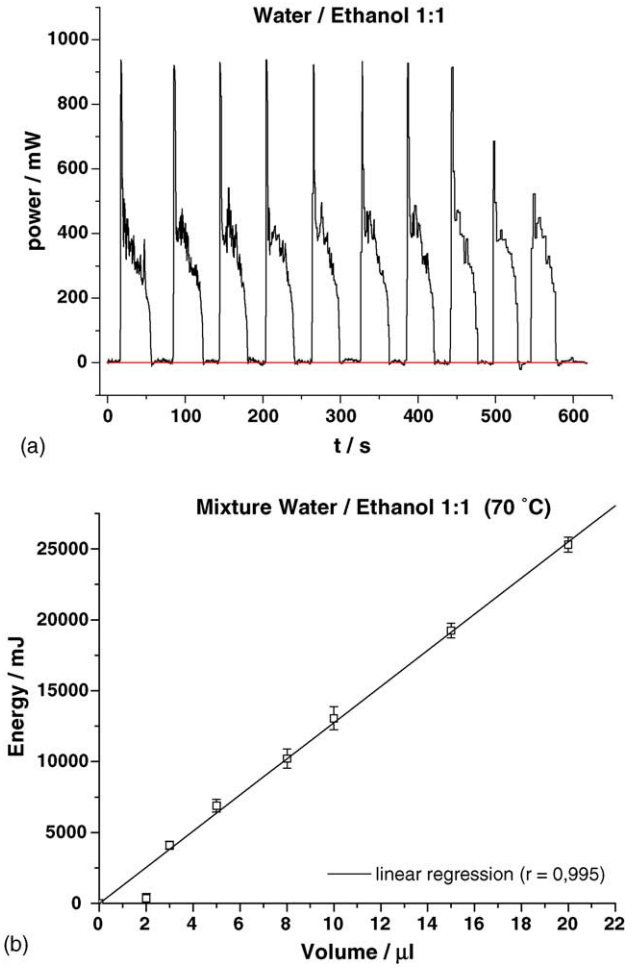

Fig. 16. Reproducibility of the evaporation experiments with binary mixtures: (a) evaporation series of a 10 μL ethanol and water (1:1) droplets and (b) consumed energy in dependence on droplet volume.

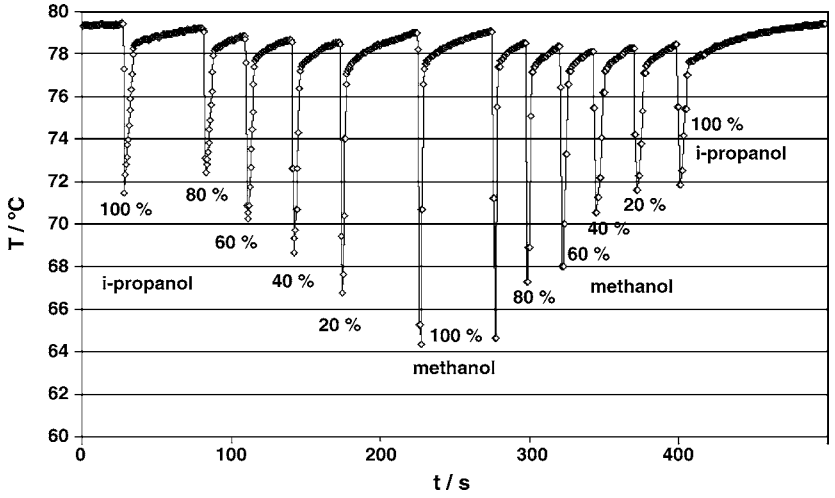

Fig. 17. Evaporation of binary mixtures: transient temperature signals of 5 μL droplets composed of two solvents (*iso*-propanol and methanol). Measured in constant power mode (1.4 W).

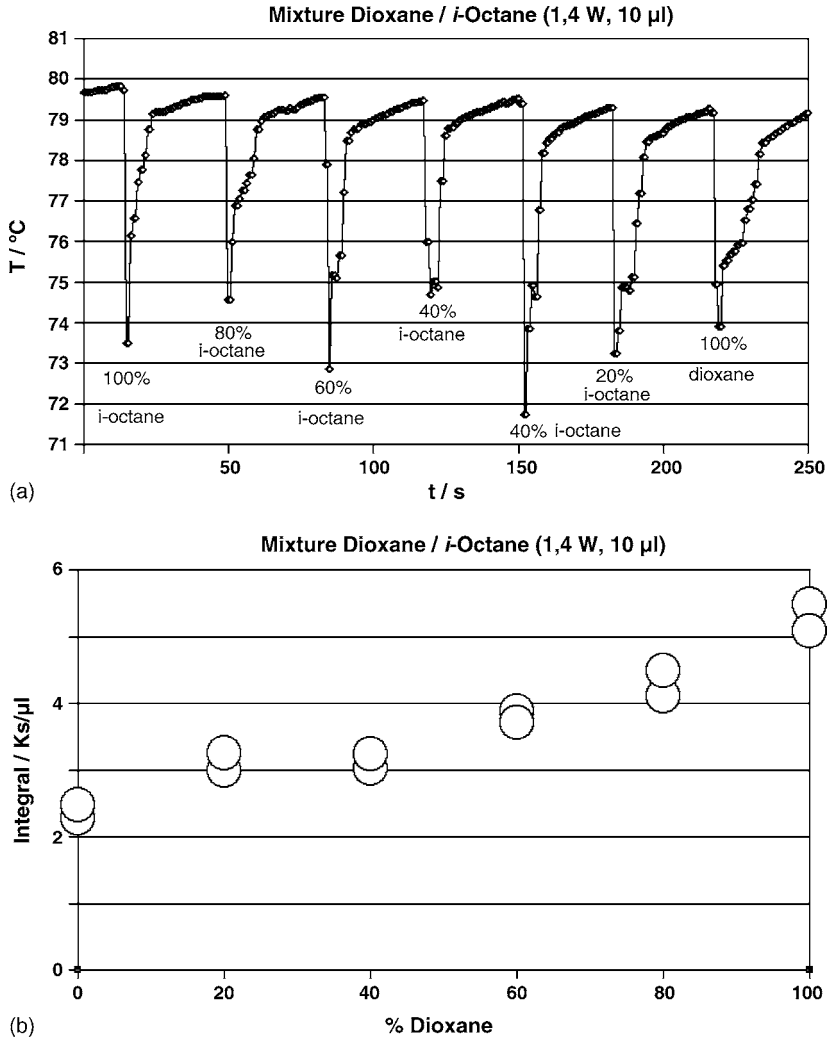

Fig. 18. Evaporation of 1,4-dioxane/*iso*-octane mixtures: (a) transient temperature signals of 5 μL droplets. Measured in constant power mode (1.4 W). (b) Integrated temperature signal of 5 μL droplets of 1,4-dioxan/*iso*-octane mixtures.

miniaturized characterization of pure solvents but also for the characterization of mixtures. Particularly the quantitative composition of binary mixtures can be characterized by microevaporation experiments. Measurements with constant power (1.4 W) were carried out for this purpose.

In water and ethanol mixtures decreases the transition time with decreasing water content (Fig. 14). This decrease is caused by the much lower evaporation enthalpy of ethanol compared to water. In contrast to transition time, the temperature deviation during the transition is only marginally influenced by the composition. The transition time is changed with concentration faster at low ethanol content and slower at higher ethanol concentrations (Fig. 15). This behaviour corresponds well to the phase transition behaviour of binary systems, in general. The reproducibility of evaporation experiments with binary mixtures of ethanol and water is shown in Fig. 16a and b.

Beside aqueous mixtures, binary mixtures of solvents with lower evaporation enthalpies can also be characterized at the 5 μL level using the chip device. A significant shift in peak amplitude and transition behaviour was observed in mixtures of *iso*-propanol and methanol. Methanol possesses a high vapour pressure and a comparatively high volume-related evaporation enthalpy, *iso*-propanol evaporates slower, but is characterized by a lower volume-related evaporation enthalpy. As a result the temperature drop increase, if the content of methanol in binary mixtures was enhanced (Fig. 17). Simultaneously, the duration of the transition is decreased due to the decreasing part of the slower evaporating solvent.

Reproducible results were obtained if the integral of temperature drop over the transition time was used for the comparison of droplets of different composition. In the system *iso*-octane/1,4-dioxane the integral was growing continuously with increasing content of 1,4-dioxane. The low volume-related evaporation enthalpy of *iso*-octane and the more than twice higher volume-related evaporation enthalpy of 1,4-dioxane are responsible for that finding (Fig. 18a and b). The dependence of the temperature-drop-time integral for octane/*iso*-propanol mixtures is also significant (Fig. 19). The observed differences correspond well to the differences of the volume-related evaporation enthalpies of the different solvents. The determination of mixture composition is possible by means of temperature measurements at constant power as well as by means of measurements of power at constant temperatures.

The temperature drop characteristic during the evaporation of droplets in constant power mode gives information about the evaporation characteristics. The maximal temperature drop depends on the vapour pressure of the applied liquid (see Fig. 20a). The vapour pressure p_v is connected with the evaporation enthalpy ΔH and the boiling temperature T_b (Eq. (1)) as outlined in Fig. 20b.

$$\ln p_v = \ln p_0 - \frac{\Delta H}{R}\left(\frac{1}{T} - \frac{1}{T_b}\right) \quad (1)$$

p_0 is the vapour pressure at T_b (1 atm).

It was expected that the temperature drop maximum increase with increasing vapour pressure like Eq. (2). This tendency is well reflected by the behaviour of different solvents like shown in Fig. 12.

$$\Delta T \sim \Delta H p_v \quad (2)$$

The integrated temperature signal I (K s/μL) at constant power mode corresponds to the consumed heating power during the evaporation process. In case of binary mixtures (x_n = volume fraction, n = 1 compound with the higher boiling

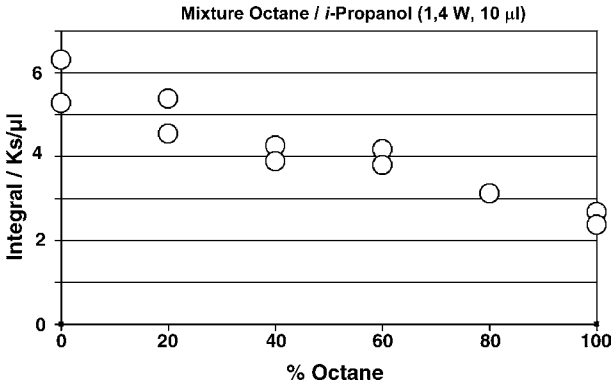

Fig. 19. Temperature transients of 5 μL droplets composed of *iso*-octane and *iso*-propanol at constant heating power of 1.4 W.

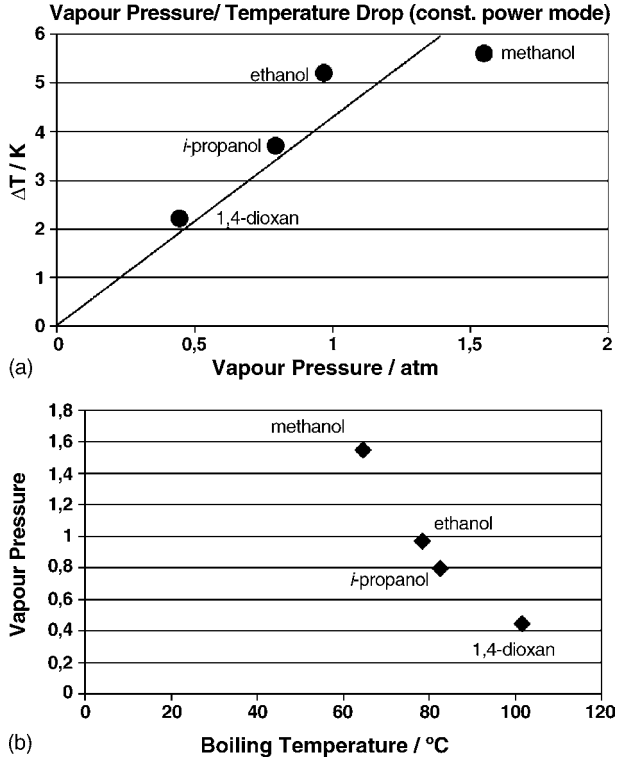

Fig. 20. (a) Experimentally observed temperature drop of different solvents in dependence of the calculated vapour pressure p_v. (b) Vapour pressure of different solvents as a function of their boiling temperatures.

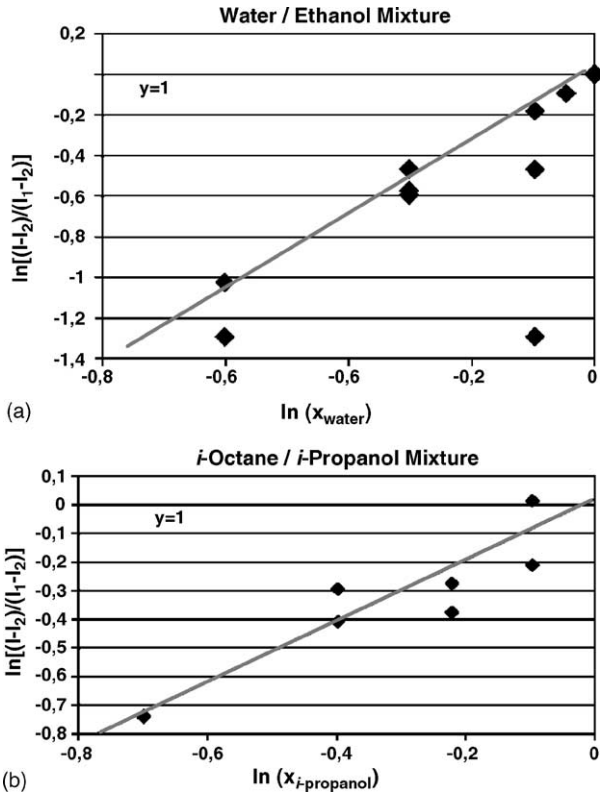

Fig. 21. (a) Determination of the exponential parameter (y) of Eqs. (3) and (4) for ethanol/water mixtures. (b) Determination of the exponential parameter (y) of Eqs. (3) and (4) for *iso*-octane/*iso*-propanol mixtures.

temperature T_b) the integrated signals can nearly be described by the empirical equation (3). I_n is the integrated temperature signal of the pure liquid:

$$I = I_1 x^y + I_2(1 - x^y) \tag{3}$$

The exponential parameter y can be determined by Eq. (4):

$$y = \frac{\ln(x)}{\ln\left[\frac{I-I_2}{I_1-I_2}\right]} \tag{4}$$

In case of the ethanol/water and *iso*-octane/ *iso*-propanol mixtures y was found to be at a value of about 1 (see Fig. 21a and b). The evaporation time Δt (transient time) can be expressed as a linear function (Eq. (5)) of the volume fraction, if y is unity, the influence of the temperature drop is neglected and a constant heating power P is applied:

$$\Delta t = [\Delta H_{vol(1)} x + \Delta H_{vol(2)}(1 - x)]\frac{1}{P} \tag{5}$$

The measurement device can easily be calibrated using known liquids or series of known liquid compositions. All shown data are raw-data. In all cases, the measurements can be carried out within a few minutes. The substance consumption is very low, because droplet volumes between 2 and 5 μL are sufficient for the measurements.

4. Summary

It was shown that the chip evaporator with integrated thin film transducers is suited for a fast characterization of the evaporation behaviour of small liquid volumes. It is possible to estimate evaporation enthalpies of solvents and binary mixtures if a simple calibration procedure is applied. The required solvent volumes are in the range between 2 and 10 μL. At a heating power of 1.4 W reproducible results were obtained in the constant power measurement mode. The thermo-resistive readout of temperature deviations allows the characterization of mixture compositions and the monitoring of the evaporation of small liquid volumes. Alternatively isothermal measurements were carried-out using temperature control by a fast feed back between the temperature depended resistance of measurement elements and the voltage applied to the thin film heaters. Process enthalpies were determined directly by integration of heating power differences over time.

Acknowledgement

For technical support, we thank M. Urban, M. Sossna, F. Jahn (IPHT Jena) and J. Wagner, M. Leich, F. Möller, P.M. Günther (TU-Ilmenau). Financial support by the DBU (German Federal Environment Foundation) is gratefully acknowledged.

References

[1] D.J. Harrison, K. Fluri, K. Seiler, Z. Fan, C.S. Effenhauser, A. Manz, Science 261 (1993) 895–897.
[2] A. Manz, D.J. Harrison, E. Verpoorte, H.M. Widmer, Adv. Chromatogr. 33 (1993) 1–66.
[3] M.T. Pham, S. Howitz, T. Hellfeld, J. Albrecht, Proceedings of the ITG "Sensoren—Technologie und Anwendung" Fachber, vol. 126, 1994, pp. 349–354.
[4] E. Verpoorte, N.F. De Rooij, Proceedings of the μ-TAS, Dordrecht, The Netherlands, Kluwer Academic Publishers, 1996, p. 16.
[5] M.A. Northrup, M.T. Ching, R.M. White, R.T. Watson, Proceedings of the Seventh International Conference on Solid-State Sensors and Actuators, 1993, pp. 924–926.
[6] M. Schena, D. Shalon, R.W. Davis, P.P. Brown, Science 270 (1995) 467–470.
[7] S.P.A. Fodor, Science 277 (1997) 393–395.
[8] R.J. Lipshutz, D. Morris, M. Chee, E. Hubbel, M.J. Kozal, N. Shah, N. Shen, R. Yang, S.P.A. Fodor, Biotechniques 19 (1995) 442–447.
[9] J.M. Köhler, U. Dillner, A. Mokansky, S. Poser, T. Schulz, Proceedings of the Second International Conference on Micoreaction Technology, New Orleans, 1998, p. 241ff.
[10] M.U. Koop, D.J. DeMello, A. Manz, Science 280 (1998) 1046–1048.
[11] Y. Baba, Proceedings of the μ-TAS, Kluwer Academic Publishers, Dordrecht, The Netherlands, 2000, p. 467.
[12] I. Schneegaß, J.M. Köhler, Rev. Mol. Biotechnol. 82 (2001) 101–121.
[13] I. Schneegaß, R. Bräutigam, J.M. Köhler, Lab. Chip 1 (2001) 42–49.

[14] A. Schober, G. Schlingloff, A. Thamm, H.J. Kiel, D. Tomandl, M. Gebinoga, M. Döring, J.M. Köhler, G. Mayer, Microsyst. Technol. 4 (1997) 35–39.
[15] E. Litborn, A. Emmer, J. Roeraade, Electrophoresis 21 (2000) 91–99.
[16] J.G.E. Gardenier, R.W. Tjerkstra, A. Van den Berg, W. Ehrfeld (Eds.), Proceedings of the Third International Conference on Microreaction Technology (IMRET 3), Springer, Berlin, 2000, p. 36.
[17] M.A. Liauw, M. Baerns, R. Broucek, O.V. Buyevskaya, J.-M. Commenge, J.-P. Corriou, K. Gebauer, H.-J. Hefter, O.-U. Langer, M. Matlosz, A. Renken, A. Rouge, R. Schenk, N. Steinfeldt, St. Walter, in: W. Ehrfeld (Ed.), Proceedings of the Third International Conference on Microreaction Technology (IMRET 3), Springer, Berlin, 2000, p. 224.
[18] J.M. Köhler, M. Zieren, Fresenius J. Anal. Chem. 358 (1997) 683–686.
[19] J. Brandner, M. Fichtner, K. Schubert, M.A. Liauw, G. Emig, Proceedings of the Fifth International Conference on Microreaction Technology (IMRET-5), vol. 5, Springer, Berlin, 2001, p. 164.
[20] (a) V. Hessel, H. Löwe, Chem. Ing. Tech. 74 (2002) 17–30;
(b) V. Hessel, H. Löwe, Chem. Ing. Tech. 74 (2002) 185–207.
[21] T. Thorsen, R.W. Roberts, F.H. Arnold, S.R. Quake, Phys. Rev. Lett. 86 (2001) 4163–4166.
[22] J.R. Burns, C. Ramshaw, Lab. Chip 1 (2001) 10–15.
[23] R. Schenk, V. Hessel, B. Werner, F. Schönfeld, Ch. Hofmann, M. Donneta, N. Jongena, Proceedings of the 15th Symposium on Industrial Crystallization, Sorrento, 2002.
[24] T. Nisisako, T. Torii, T. Higuchi, Lab. Chip 2 (2002) 24–26.
[25] T. Taniguchi, T. Torii, T. Higuchi, Lab. Chip 2 (2002) 19–23.
[26] A. Grodrian, J. Metze, Th. Henkel, M. Roth, J.M. Köhler, Proceedings of the SPIE Symposium on Smart Materials, Nano- and Micro Smart Systems, 4937, 2002, pp. 174–181.
[27] H. Song, J.D. Tice, R.F. Ismagilov, Angew. Chem. 115 (2003) 792–796.
[28] J.M. Köhler, A. Schober, A. Schwienhorst, Exp. Technol. Phys. 40 (1994) 35–56.
[29] A. Schober, A. Schwienhorst, J.M. Köhler, M. Fuchs, R. Günther, M. Thürk, Microsyst. Technol. 1 (1995) 168–172.
[30] G. Mayer, A. Schober, J.M. Köhler, Rev. Mol. Biotechnol. 82 (2001) 137–159.
[31] G. Mayer, K. Wohlfahrt, A. Schober, J.M. Köhler, Nanotiterplates for Screening and Synthesis, in: J.M. Köhler, T. Mejevaia, H. Saluz (Eds.), Micro System Technology: A Powerful Tool for Biomolecular Studies, Birkhäuser, Basel, 1999, pp. 75–128.
[32] D'Ans Lax, in: E. Lax, C. Synowietz (Eds.), Taschenbuch für Chemiker und Physiker, Bd II, Springer-Verlag, Berlin, 1964.